JOC The Journal of Organic Chemistry

Article

pubs.acs.org/joc

Triple Shifts and Thioether Assistance in Rearrangements Associated with an Unusual Biomethylation of the Sterol Side Chain

Young J. Hong,[‡] José-Luis Giner,[†] and Dean J. Tantillo*[,‡]

[‡]Department of Chemistry, University of California—Davis, 1 Shields Avenue, Davis, California 95616, United States

[†]Department of Chemistry, State University of New York-ESF, 1 Forestry Drive, Syracuse, New York 13210, United States

Supporting Information

ABSTRACT: Quantum chemical calculations (B3LYP and MP2) are described for the formation and rearrangements of carbocations derived from the biological methylation reaction that produces 24-propyl sterols in pelagophyte algae. Previous mechanistic proposals are discussed in light of the results of these calculations. Of particular note is the prediction of a new triple-shift rearrangement that is inherently preferred for the biosynthetically relevant carbocations. Our calculations also reveal how these reactions may be affected by intermolecular interactions with *S*-adenosylmethionine.

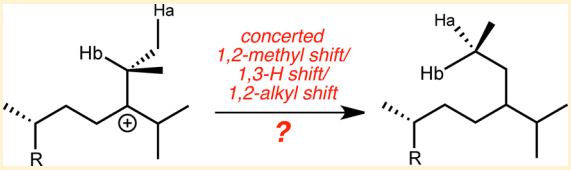

INTRODUCTION

The side chains of sterols are often elaborated *via* hydrogenation, dehydrogenation, and methylation, and various mechanistically interesting cationic rearrangements occur during their biosynthesis.[1,2] For example, in pelagophyte algae, the enzymatic reaction of isofucosterol (**1**) with *S*-adenosylmethionine (SAM) leads to 24-propylidenecholesterol (**3**), together with the minor products depicted in Scheme 1.[3] This is in contrast to the mechanistically more commonplace outcome in sponges and orchids where 24-isopropyl sterols (e.g., **4**) are formed.[4] Based on the co-occurrence of cyclopropyl sterol **2** and the results of isotopic labeling experiments, mechanisms for the formation of **3** involving protonated cyclopropane intermediates (Scheme 2, black arrows; **B** is a protonated cyclopropane) have been proposed.[1,3c−e] Herein we describe the results of quantum chemical calculations (both density functional theory (DFT) and MP2 calculations[5−12]) on mechanisms leading from **1** to **2**−**6**.[13] On the basis of these results, we suggest a modified mechanistic picture that involves a protonated cyclopropane as a transition state structure rather than an intermediate and several steps in which two or three alkyl or hydride shifting events are merged into concerted processes (Scheme 2, red arrows).[14] We also examine the potential roles of the thioether left behind after the transfer of the SAM methyl group.

Scheme 1

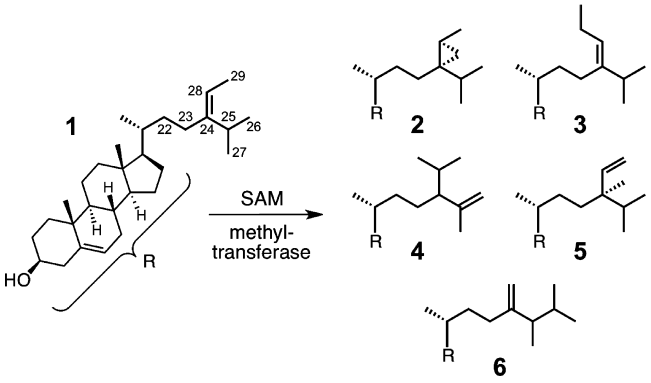

RESULTS AND DISCUSSION

Our calculations involved, as a starting point, a model (**A1**, Figure 1) of the classical tertiary carbocation (carbenium ion) derived from CH_3^+-transfer to **1** (**A**, Scheme 2) in which the steroid nucleus and two adjacent carbons of the side chain of carbocation **A** were replaced by hydrogen (all model cations are named using the letters in Scheme 2 followed by the number 1; calculations in the absence of an enzyme).[15,16] Using this model, **A** → **C** (precursor to **3**), **A** → **D** (precursor to **4**), and **A** → **F** (precursor to **6**) rearrangements were examined.

As shown at the top of Figure 1, the conversion of **A1** to **C1** is computed to be a concerted process in which three events, 1,2-methyl shift (C30 from C28 to C24), 1,3-hydride shift (from C30 to C28), and 1,2-ethyl shift (C28 from C24 to C30), are merged into a single step with no intermediates.[14] These three events occur asynchronously, with the methyl shift occurring early and the ethyl shift late, as shown by the results of intrinsic reaction coordinate calculations; the same process was observed when using B3LYP or MP2 calculations (Figure 2).[17] These calculations indicate that the biosynthetic reaction should involve structures resembling secondary and primary carbocations along the pathway, but not as intermediates (**E** and **H** in Scheme 3). A similar triple-shift reaction was described previously as part of the biosynthesis of atiserene, a polycyclic diterpene.[18]

The transition state structure for this triple-shift reaction (Figures 1 and 2) actually resembles the previously proposed edge-protonated cyclopropane intermediate (**B**, Scheme 2).[1,3d,e,19]

Received: November 1, 2012
Published: December 27, 2012

   dx.doi.org/10.1021/jo3024208 | *J. Org. Chem.* 2013, 78, 935−941

Scheme 2[a]

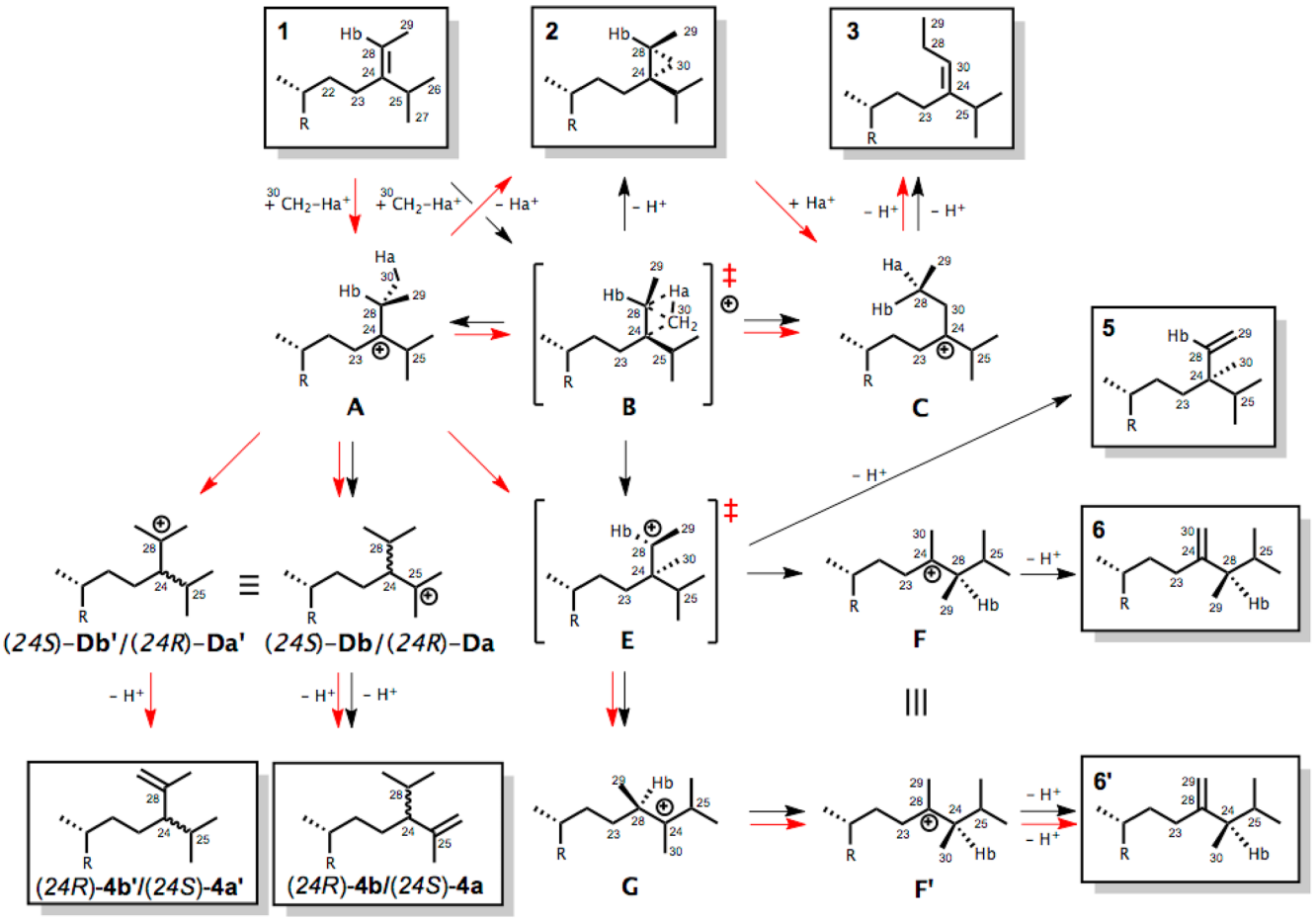

[a]Atom numbering throughout is based on that for structure **1**. Note that **F** and **F′** are equivalent only in the absence of atom labeling.

Figure 3a shows the charge distribution in this transition state structure from two views; clearly H_a (the bridging hydrogen) and the C30 methylene group are the most positive regions of this structure. Figure 3b shows computed chemical shifts for the various protons and carbons in the transition state structure. Although these are not simple to interpret,[20] it is clear that C30 is the most electron-deficient of the three carbons involved in the triple shift (C24, C30, and C28). Taken together, the charge distribution and chemical shifts suggest that a resonance structure containing a primary cation substructure actually contributes significantly to the electronic structure of the transition state.

Our calculations on the proposed biosynthesis of sterol **6** (Scheme 2) indicate that the conversion of **A** to **F′** also involves an interesting reaction that avoids a previously proposed intermediate. We have found a concerted reaction in which **A1** is converted directly to **G1** (Figure 1) and **E** is not an intermediate but rather appears to be a transition state structure for the **A1**-to-**G1** reaction. This process involves the asynchronous combination of two alkyl shifts (C30 from C28 to C24 and C23 from C24 to C28; Figure 4), an example of an asynchronous dyotropic rearrangement.[21] Several recent theoretical studies have revealed similar dyotropic rearrangements that avoid the formation of secondary carbocations as intermediates in biosynthetic pathways to terpene natural products and instead have transition state structures resembling secondary carbocations.[9a,10b,14,18,21f,22] Carbocation **G1** then undergoes a simple, low-barrier 1,2-hydride shift to form **F1′** (Figure 1).[23] Note

Scheme 3

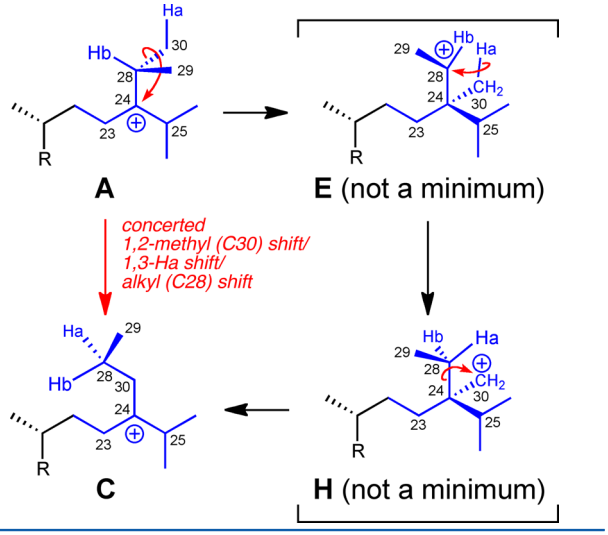

that in our proposed reaction network (Scheme 2, red arrows), cation **F** is not formed. This prediction, that **F′** rather than **F** should precede **6**, could be tested by appropriate labeling studies.[24] Note also that **E1** = **TS (A1−G1)** is very similar in structure to the **E1**-like species involved in the **A1** → **C1** reaction (Figure 2 and Scheme 3), suggesting that there may be a bifurcation along the path uphill from **A1** toward **TS (A1−C1)**.[25]

dx.doi.org/10.1021/jo3024208 | J. Org. Chem. 2013, 78, 935−941

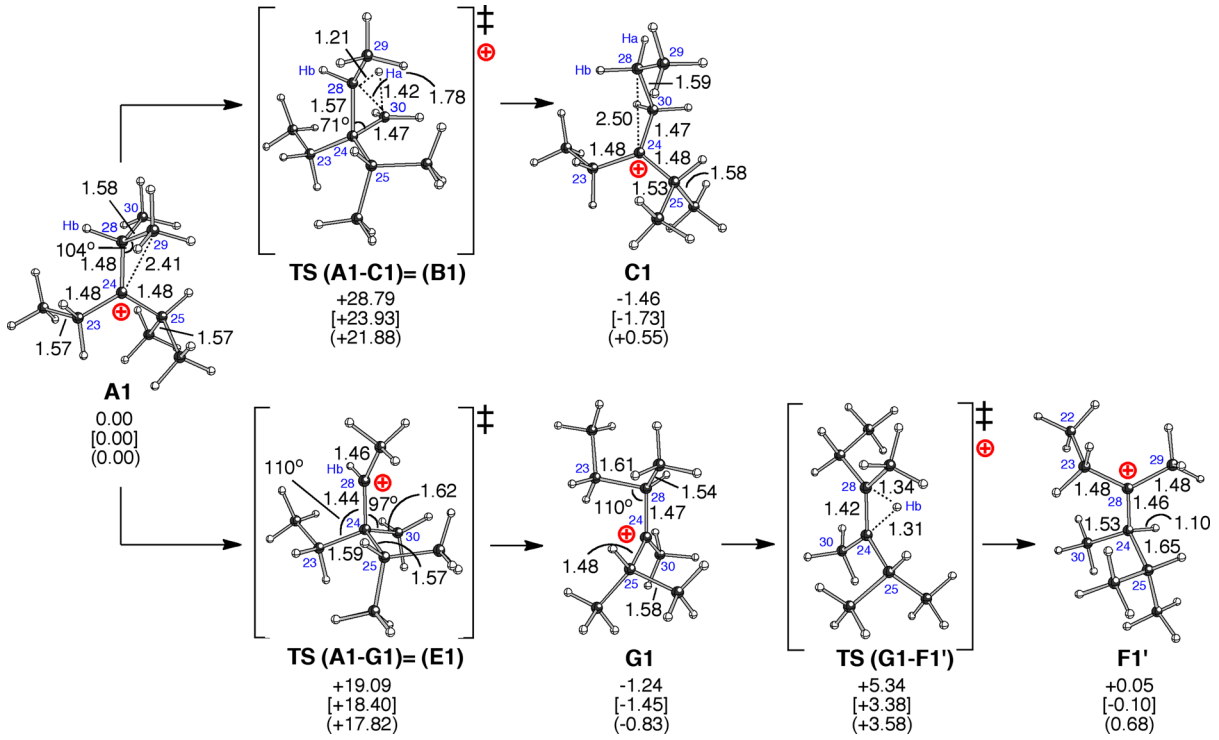

Figure 1. A1 to **C1** and **F1′** rearrangements. Computed geometries (distances in Å, B3LYP/6-31+G(d,p)) and energies (kcal/mol, relative to that of **A1**, B3LYP/6-31+G(d,p)//B3LYP/6-31+G(d,p) in normal text, mPW1PW91/6-31+G(d,p)//B3LYP/6-31+G(d,p) in brackets, MP2/6-31+G(d,p)//B3LYP/6-31+G(d,p) in parentheses) of intermediates and transition state structures are shown.

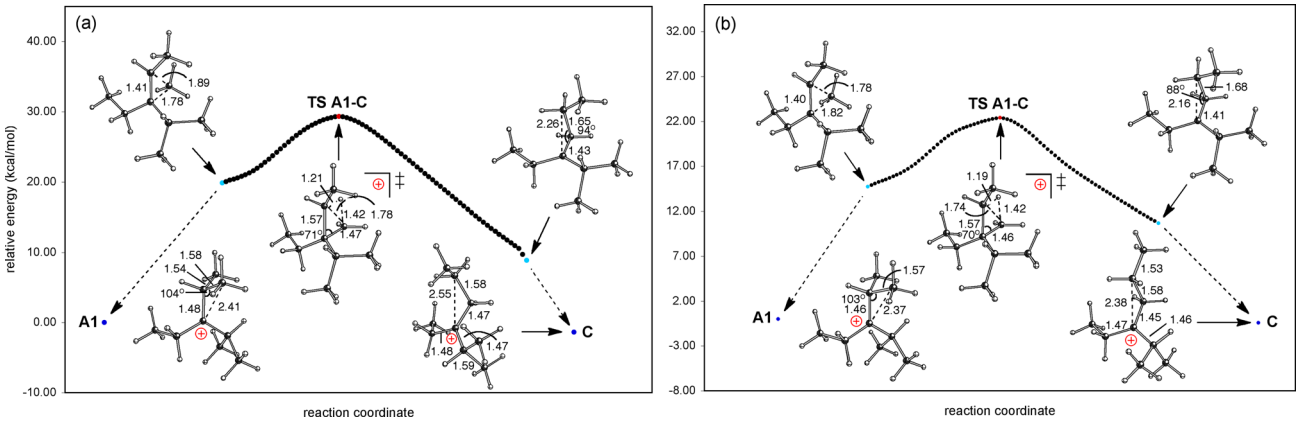

Figure 2. Conversion of **A1** to **C** from IRC calculations using (a) the B3LYP/6-31+G(d,p) method and (b) the MP2/6-31+G(d,p) method. Energies do not include zero-point energy corrections.

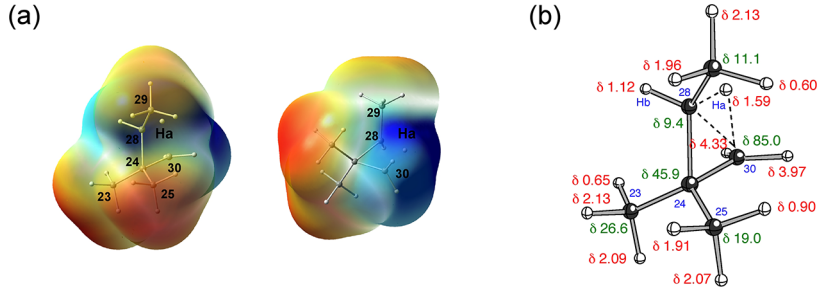

Figure 3. (a) Electrostatic potential surface (2 views) of a small model of **TS A1-C1** (B3LYP/6-31+G(d,p)) without the isopropyl group. Red areas are least positive, and blue areas are most positive (range, +0.123 to +0.183 au). (b) Computed (B3LYP/6-311+G(d,p)//B3LYP/6-31+G(d,p)) chemical shifts (relative to TMS): ^{1}H in red and ^{13}C in green.

The formation of various stereoisomers of carbocation **D** from **A** *via* simple 1,2-hydride shifts for various conformers of **A** (see Supporting Information for details) is predicted to involve only low barriers (<9 kcal/mol) and so should occur readily in an

dx.doi.org/10.1021/jo3024208 | J. Org. Chem. 2013, 78, 935−941

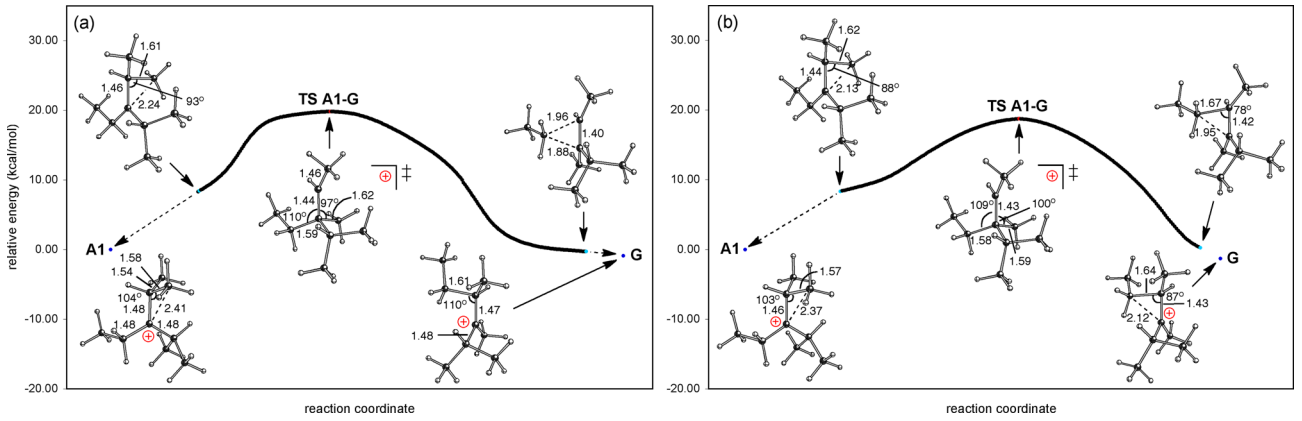

Figure 4. Conversion of **A1** to **G1** from IRC calculations using (a) the B3LYP/6-31+G(d,p) method and (b) the MP2/6-31+G(d,p) method. Energies do not include zero-point energy corrections.

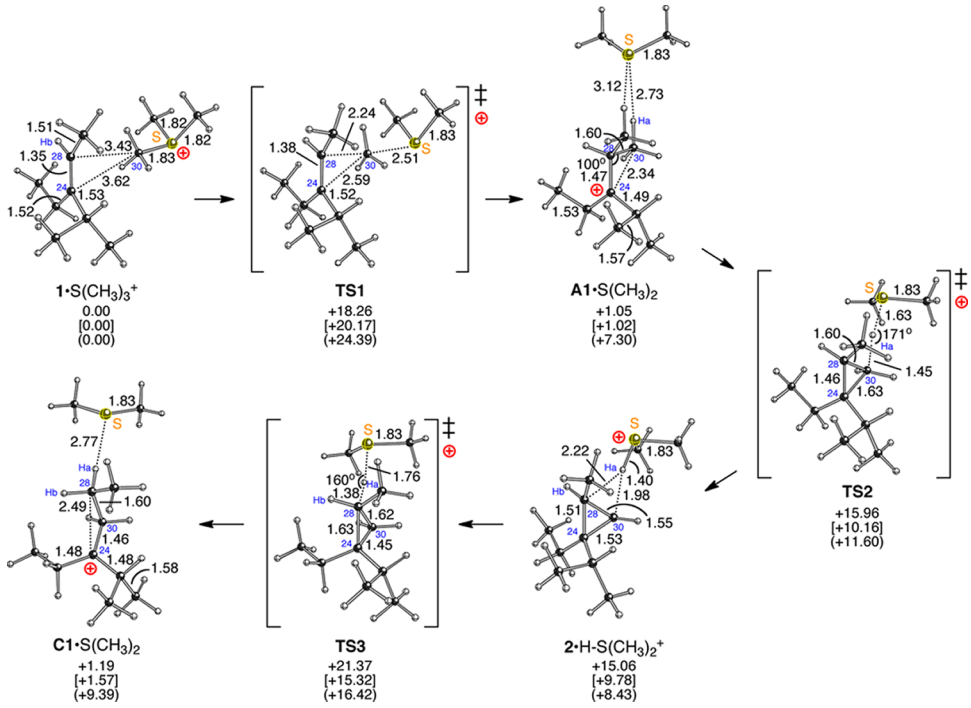

Figure 5. **1** to **A1** to **C1** reaction in the presence of $S(CH_3)_2$. Computed geometries (distances in Å, B3LYP/6-31+G(d,p)) and energies (kcal/mol, relative to that of **1**·$S(CH_3)_3^+$, B3LYP/6-31+G(d,p)//B3LYP/6-31+G(d,p) in normal text, mPW1PW91/6-31+G(d,p)//B3LYP/6-31+G(d,p) in brackets, MP2/6-31+G(d,p)//B3LYP/6-31+G(d,p) in parentheses) of intermediates and transition state structures are shown. **1**·$S(CH_3)_3^+$ has a small imaginary frequency (-6.97 cm^{-1}) associated with $S(CH_3)_3^+$ movement, and several similar complexes were located that also have small imaginary frequencies. The relative energies of these complexes are very similar, however, and we suspect that the potential energy surface in this region is rather flat (see Supporting Information for details).

enzyme active site, although which particular conformer reacts, if any, could be controlled by preorganizing the conformation of **A**. These 1,2-shifts are also predicted to be readily reversible, since none are predicted to be significantly exothermic (in fact, most are predicted to be endothermic by several kcal/mol).[26] However, factors that favor the olefinic products of cation **D** over those of cation **A** include less hindered approach of the base and a greater number of hydrogens available for deprotonation.

The computed barrier for the **A**-to-**C** reaction (Figure 1) is a bit high for a biological reaction (although this barrier could be lowered in an enzyme active site), so we considered the possibility of an alternative deprotonation/reprotonation mechanism. Since **A** would be formed *via* methyl transfer from SAM,[27] demethylated SAM (*S*-adenosylhomocysteine, SAH) should be in the vicinity of enzyme-generated **A**, and this thioether could, in principle, facilitate proton transfer. This possibility was examined using $S(CH_3)_2$ as a model of SAH. Figure 5 shows computed structures for the two-step proton transfer pathway (**A1**·$S(CH_3)_2$ to **C1**·$S(CH_3)_2$), as well as the methyl transfer process that leads to **A1**.[28] Although the barrier for the methyl transfer step is again a bit high (but again could be lowered in an enzyme active site), the overall barrier for the proton transfer process is significantly lower than that for the direct **A1**-to-**C1** reaction. Note that in the 2-step process, intermediate cyclopropane **2** (Schemes 1 and 2) is formed by a concerted deprotonation/cyclization.[29]

dx.doi.org/10.1021/jo3024208 | *J. Org. Chem.* 2013, 78, 935−941

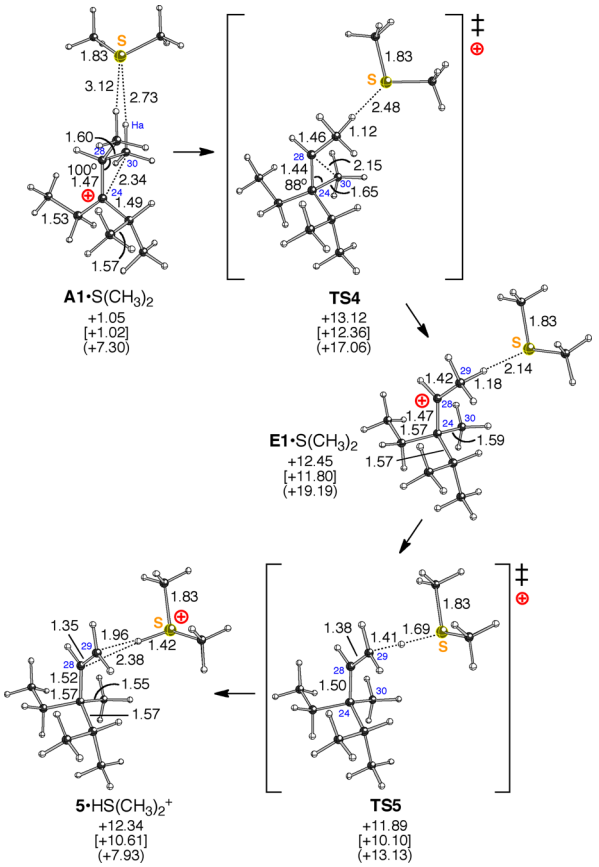

Figure 6. **A1** to **5** reaction in the presence of $S(CH_3)_2$. Computed geometries (distances in Å, B3LYP/6-31+G(d,p)) and energies (kcal/mol, relative to that of **1**·$S(CH_3)_3^+$ (Figure 5), B3LYP/6-31+G(d,p)//B3LYP/6-31+G(d,p) in normal text, mPW1PW91/6-31+G(d,p)//B3LYP/6-31+G(d,p) in brackets, MP2/6-31+G(d,p)//B3LYP/6-31+G(d,p) in parentheses) of intermediates and transition state structures are shown. B3LYP and mPW1PW91 energies of **TS5** are lower than that of **5**·$HS(CH_3)_2^+$ due to zero point energy corrections. At the MP2 level, secondary cation complex **E1**·$S(CH_3)_2$ is predicted to have a higher energy than **TS4** and **TS5**.

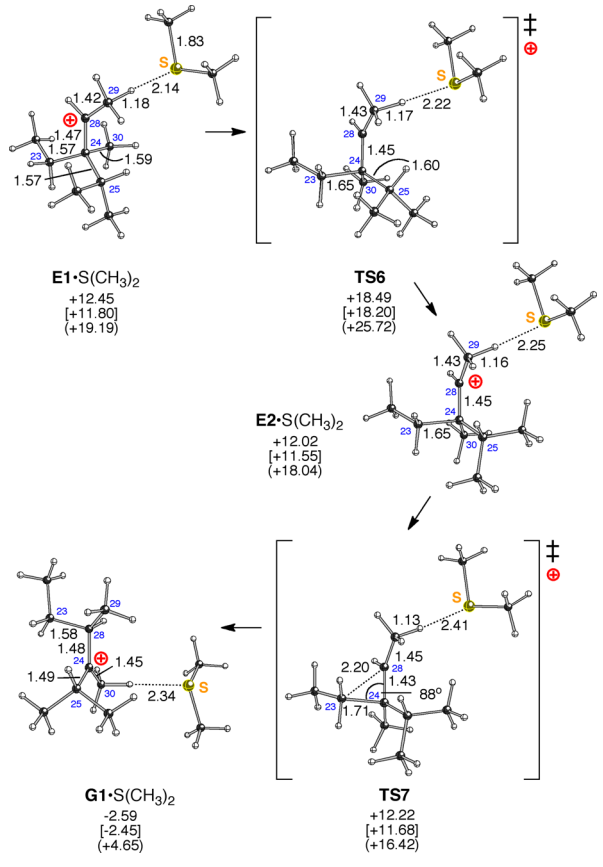

Figure 7. **E1** to **G1** reaction in the presence of $S(CH_3)_2$. Computed geometries (distances in Å, B3LYP/6-31+G(d,p)) and energies (kcal/mol, relative to that of **1**·$S(CH_3)_3^+$ (Figure 5), B3LYP/6-31+G(d,p)//B3LYP/6-31+G(d,p) in normal text, mPW1PW91/6-31+G(d,p)//B3LYP/6-31+G(d,p) in brackets, MP2/6-31+G(d,p)//B3LYP/6-31+G(d,p) in parentheses) of intermediates and transition state structures are shown. The MP2 energy of **TS7** is predicted to be lower than that of **E2**·$S(CH_3)_2$.

In addition to perturbing the **A**-to-**C** pathway, a nearby thioether can also perturb the **A**-to-**G** pathway. As shown in Figure 6, secondary carbocation **E**, which was a transition state structure in the direct **A**-to-**G** pathway (Figure 1), appears to be a minimum in the presence of $S(CH_3)_2$ due to enhanced hyperconjugation between one C29−H bond and the carbocation center at C28 as electron density is donated by sulfur (compare the C28−C29 distances for **E1** and **E1**·$S(CH_3)_2$ in Figures 1 and 6). However, this structure is very close in energy to the transition state structure that leads to it. The **E1**·$S(CH_3)_2$ complex is actually slightly higher in energy than the transition state structure for deprotonation to form **5** (**TS5**) when zero point energy is accounted for and is also very close in energy to the **5**·$HS(CH_3)_2^+$ complex. Clearly, this region of the potential energy surface is rather flat. Note also that the formation of **5** is predicted to be an uphill process that should be readily reversible if the protonated thioether remains close.

In the presence of $S(CH_3)_2$, **E1** can also be rerouted to **G1** and **F1** with lower barriers (Figures 7 and 8, respectively). Conversion to **G1** (Figure 7) is predicted to be accompanied by a higher barrier than is deprotonation to form **5** (Figure 6), by virtue of the **E1**-to-**E2** conformational change,[30] but is a significantly exothermic process. Conversion of **E1** to **F1** (Figure 8) is not predicted to have a significant barrier, however, and is again an exothermic process (although **F1**·$S(CH_3)_2$ and **A1**·$S(CH_3)_2$, Figure 6, are similar in energy). As is the case for all of these models, application to the biosynthetic reaction assumes that conformational changes, in this case to form **E2** and **E3**, are accommodated by the enzyme active site.

CONCLUSIONS

Thus, the situation is complicated. First, our prediction that **F′** should be formed preferentially over **F** does not hold when a thioether is present. Second, the potential energy surface surrounding cation **E**, when a thioether is present, is predicted to be quite flat, allowing for the product distribution to be controlled by rigid conformational constraints imposed by the enzyme and/or dynamic effects.[26,31]

The possibility that the thioether (SAH) generated during the enzymatic SAM-dependent methyl transfer reaction is involved in deprotonating an intermediate carbocation cannot easily be ruled out and is quite likely to occur in the formation of cyclopropyl sterol **2**. However, it has been shown using chirally labeled methyl groups that methylation and deprotonation occur from opposite sides of the double bond in the formation of the 24-methylene sterol side chain and tuberculostearic acid.[32]

dx.doi.org/10.1021/jo3024208 | J. Org. Chem. 2013, 78, 935−941

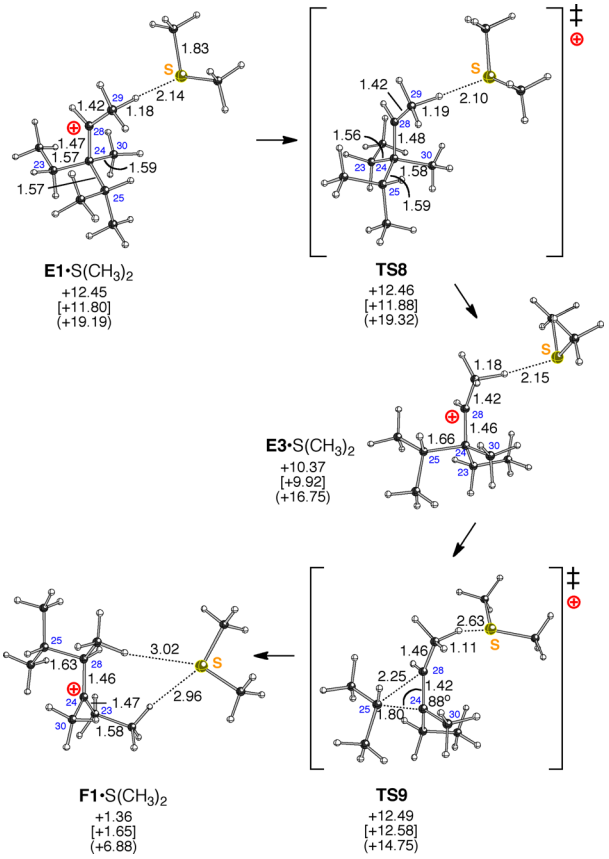

Figure 8. **E1** to **F1** reaction in the presence of $S(CH_3)_2$. Computed geometries (distances in Å, B3LYP/6-31+G(d,p)) and energies (kcal/mol, relative to that of **1**·$S(CH_3)_3^+$ (Figure 5), B3LYP/6-31+G(d,p)//B3LYP/6-31+G(d,p) in normal text, mPW1PW91/6-31+G(d,p)//B3LYP/6-31+G(d,p) in brackets, MP2/6-31+G(d,p)//B3LYP/6-31+G(d,p) in parentheses) of intermediates and transition state structures are shown. The MP2 energy of **TS9** is predicted to be lower than that of **E3**·$S(CH_3)_2$.

On the whole, we have provided energetic and structural details for species that may be involved in the biosynthesis of sterol side chains, thereby delineating a framework for future experimental design. We look forward to our predictions being put to the test by bioorganic chemists, structural biologists and mechanistic enzymologists.

■ ASSOCIATED CONTENT

Supporting Information

Coordinates and energies for all computed structures, additional details on computations not discussed at length in the text, and full Gaussian citation. This material is available free of charge via the Internet at http://pubs.acs.org.

■ AUTHOR INFORMATION

Corresponding Author

*E-mail: djtantillo@ucdavis.edu.

Notes

The authors declare no competing financial interest.

■ ACKNOWLEDGMENTS

We gratefully acknowledge the National Science Foundation (CHE-0449845, CHE-0957416, and CHE-030089 [supercomputer support]).

■ REFERENCES

(1) Giner, J.-L. *Chem. Rev.* **1993**, *93*, 1735−1752.

(2) Giner, J.-L.; Buzek, P.; Schleyer, P. v. R. *J. Am. Chem. Soc.* **1995**, *117*, 12871−12872.

(3) (a) Rohmer, M.; Kokke, W. C. M. C.; Fenical, W.; Djerassi, C. *Steroids* **1980**, *35*, 219−231. (b) Kokke, W. C. M. C.; Shoolery, J. N.; Fenical, W.; Djerassi, C. *J. Org. Chem.* **1984**, *49*, 3742−3752. (c) Giner, J.-L.; Zimmerman, M. P.; Djerassi, C. *J. Org. Chem.* **1988**, *53*, 5895−5902. (d) Giner, J.-L.; Djerassi, C. *J. Am. Chem. Soc.* **1991**, *113*, 1386−1393. (e) Giner, J.-L.; Zhao, H.; Boyer, G. L.; Satchwell, M. F.; Andersen, R. A. *Chem. Biodiversity* **2009**, *6*, 1111−1130.

(4) (a) Hofheinz, W.; Oesterhelt, G. *Helv. Chim. Acta* **1979**, *62*, 1307−1309. (b) Kokke, W. C. M. C.; Pak, C. S.; Fenical, W.; Djerassi, C. *Helv. Chim. Acta* **1979**, *62*, 1310−1318. (c) Makar'eva, T. N.; Shubina, L. K.; Kalinovskii, A. I.; Stonik, V. A.; Elyakov, G. B. *Steroids* **1983**, *42*, 267−281. (d) Kikuchi, T.; Kadota, S.; Suehara, H.; Namba, T. *Chem. Pharm. Bull.* **1985**, *33*, 2235−2242. (e) Stoilov, I. L.; Thompson, J. E.; Djerassi, C. *Tetrahedron* **1986**, *42*, 4147−4155. (f) Calderon, G. J.; Castellanos, L.; Duque, C.; Echigo, S.; Hara, N.; Fujimoto, Y. *Steroids* **2004**, *69*, 93−100.

(5) (a) All calculations were performed with GAUSSIAN03.[6] Structures were optimized using the B3LYP/6-31+G(d,p)[7] or MP2/6-31+G(d,p)[8] method. Previous studies have suggested that the B3LYP method performs reasonably well in predicting geometries and reactivity of carbocations, and results using this method have been compared with other DFT and non-DFT methods.[9] MP2 is a fundamentally different theoretical method thought to have an accuracy similar to that of B3LYP whose occassional problems are different from those of B3LYP, so when the two methods agree we feel confident that our results are reasonable.[10] As has been done in many previous studies, we report mPW1PW91/6-31+G(d,p)//B3LYP/6-31+G(d,p) energies for our DFT calculations to avoid a well-known tendency of B3LYP to underestimate the stability of cyclic structures compared to acyclic isomers.[9a,10b] All stationary points were characterized by frequency calculations and reported energies include zero-point energy corrections (unscaled) from the method used for geometry optimization. Intrinsic reaction coordinate (IRC) calculations were used for further characterization of all transition state structures,[11] and IRC plots for all transtion state structures are shown in the text or in the Supporting Information. Structural drawings were produced using Ball & Stick.[12] Atom numbering indicated in the structures in this report is based on that of **3** (Scheme 2).

(6) Frisch, M. J. et al. *Gaussian03, revision D.01*; Gaussian, Inc.: Pittsburgh, PA, 2003 (full reference in Supporting Information).

(7) (a) Becke, A. D. *J. Chem. Phys.* **1993**, *98*, 5648−5652. (b) Becke, A. D. *J. Chem. Phys.* **1993**, *98*, 1372−1377. (c) Lee, C.; Yang, W.; Parr, R. G. *Phys. Rev. B* **1988**, *37*, 785−789. (d) Stephens, P. J.; Devlin, F. J.; Chabalowski, C. F.; Frisch, M. J. *J. Phys. Chem.* **1994**, *98*, 11623−11627.

(8) (a) Hehre, W. J.; Radom, L.; Schleyer, P. v. R.; Pople, J. A. *Ab Initio Molecular Orbital Theory*; John Wiley & Sons: New York, 1986. (b) Møller, C.; Plesset, M. S. *Phys. Rev.* **1934**, *46*, 618−622.

(9) For leading references, see: (a) Tantillo, D. J. *Nat. Prod. Rep.* **2011**, *28*, 1035−1053. (b) Hess, B. A., Jr.; Smentek, L. *Collect. Czech. Chem. Commun.* **2008**, *73*, 786−794.

(10) Recent examples of comparisons between B3LYP and MP2 for carbocation structures and reactions: (a) Reference 9a. (b) Matsuda, S. P. T.; Wilson, W. K.; Xiong, Q. *Org. Biomol. Chem.* **2006**, *4*, 530−543.

(11) (a) Gonzalez, C.; Schlegel, H. B. *J. Phys. Chem.* **1990**, *94*, 5523−5527. (b) Fukui, K. *Acc. Chem. Res.* **1981**, *14*, 363−368.

(12) Müller, N.; Falk, A.; Gsaller, G. *Ball & Stick V.4.0a12, molecular graphics application for MacOS computers*; Johannes Kepler University: Linz, 2004.

(13) Rearrangements of related carbocations, produced during metalloenzyme-promoted dehydrogenation of clionasterol, were examined previously using HF and MPn calculations. See ref 2.

(14) For leading references on concerted but asynchronous combinations of bond-making and -breaking events in carbocation rearrangements relevant to terpene biosynthesis, see: (a) Tantillo, D. J. *Chem. Soc. Rev.* **2010**, *39*, 2847−2854. (b) Tantillo, D. J. *J. Phys. Org.*

Chem. **2008**, *21*, 561−570. (c) Reference 9a. (d) A seminal paper of relevance to terpene biosynthesis Hess, B. A., Jr. *J. Am. Chem. Soc.* **2002**, *124*, 10286−10287.

(15) A smaller model system with methyl groups in place of the ethyl and one of the isopropyl groups was also examined and very similar results were obtained. See Supporting Information for details.

(16) Alternatively, one could recast the mechanistic discussion starting with **B** or **E** or alkene **1** + $H_3CSR_2^+$, but as discussed later, **B** and **E** appear to be transition state structures, and (we feel) the role of SAM is clarified through comparisons to carbocation systems lacking thioether models.

(17) The analogue of Figure 1 showing MP2 geometries can be found in the Supporting Information

(18) (a) Hong, Y. J.; Tantillo, D. J. *J. Am. Chem. Soc.* **2010**, *132*, 5375−5386. (b) Hong, Y. J.; Ponec, R.; Tantillo, D. J. *J. Phys. Chem. A* **2012**, *116*, 8902−8909.

(19) Interesting discussions of edge-protonated cyclopropanes include: (a) Saunders, M.; Vogel, P.; Hagen, E. L.; Rosenfeld, J. *Acc. Chem. Res.* **1973**, *6*, 53−59. (b) Collins, C. J. *Chem. Rev.* **1969**, *69*, 543−550.

(20) (a) For a recent review on the use of computational chemical shifts of carbocations, see: Siehl, H.-U. *Adv. Phys. Org. Chem.* **2008**, *42*, 125−165. (b) For a general review on NMR chemical shift computations, see: Lodewyk, M. W.; Siebert, M. R.; Tantillo, D. J. *Chem. Rev.* **2012**, *112*, 1839−1862.

(21) (a) Reetz, M. T. *Angew. Chem., Int. Ed. Engl.* **1972**, *11*, 130−131. (b) Reetz, M. T. *Angew. Chem., Int. Ed. Engl.* **1972**, *11*, 129−130. (c) Reetz, M. T. *Tetrahedron* **1973**, *29*, 2189−2194. (d) Reetz, M. T. *Adv. Organomet. Chem.* **1977**, *16*, 33−65. (e) Fernandez, I.; Cossio, F. P.; Sierra, M. A. *Chem. Rev.* **2009**, *109*, 6687−6711. (f) Gutierrez, O.; Tantillo, D. J. *J. Org. Chem.* **2012**, *77*, 8845−8850.

(22) (a) Hong, Y. J.; Tantillo, D. J. *Nat. Chem.* **2009**, *1*, 384−389. (b) Hong, Y. J.; Tantillo, D. J. *J. Am. Chem. Soc.* **2009**, *131*, 7999−8015.

(23) At the MP2/6-31+G(d,p) level, a bridged intermediate between **G1** and **F1′** was located, but once zero-point energy is accounted for, this intermediate is actually slightly higher in energy than the transition state structures that flank it. This implies that the potential energy surface between **G1** and **F1′** (i.e., near **TS (G1−F1′)** in Figure 1) is somewhat flat with respect to sliding of the hydrogen between C24 and C28.

(24) (a) Labeling C24, C28, C29 and/or C30 (see Scheme 2) would provide evidence for or against our proposal. (b) The preferential migration of the less substituted group (C23 to C28 instead of C25 to C28) is not uncommon in isoprenoid cationic rearrangements.[1,9a]

(25) Leading references on (downhill) bifurcations: (a) Reference 22. (b) Ess, D. H.; Wheeler, S. E.; Iafe, R. G.; Xu, L.; Çelebi-Ölçüm, N.; Houk, K. N. *Angew. Chem., Int. Ed.* **2008**, *47*, 7592−7601.

(26) Related examples of proposed equilibration before deprotonation in terpene/terpenoid biosynthesis: (a) Hong, Y. J.; Tantillo, D. J. *J. Am. Chem. Soc.* **2011**, *133*, 18249−18256. (b) Sio, V.; Harrison, J. G.; Tantillo, D. J. *Tetrahedron Lett.* **2012**, *53*, 6919−6922.

(27) While we cannot definitively rule out formation of an alternative carbocation that rearranges to the observed products, our calculations suggest that **A** is a reasonable intermediate. Even if **A** is formed via rearrangement of a different species, it is likely that demethylated SAM (SAH) would be nearby.

(28) The relative positions of carbocations formed in the enzyme active site and demethylated SAM (SAH) are likely to be more constrained than in our calculations (we did not impose any constraints; Figure 5 shows fully optimized structures). Nonetheless, our calculations reveal the types of interactions that may occur and the inherent barriers for various reaction steps; an enzyme could, in principle, raise or lower these barriers.

(29) A deprotonation/reprotonation sequence with ammonia as the base was also examined; see Supporting Information for details. See also ref 9a for related examples.

(30) Note that the conversion of **E1** to **E2** via **TS6** involves two rotations about the C24−C28 and C24−C25 bonds. Reorientation of the isopropyl group prevents a steric clash with the ethyl group in the subsequent ethyl shift reaction.

(31) For leading references, see: (a) Carpenter, B. K. *Annu. Rev. Phys. Chem.* **2005**, *56*, 57−89. (b) A recent example related to terpene biosynthesis: Siebert, M. R.; Paranjothy, M.; Sun, R.; Tantillo, D. J.; Hase, W. L. *J. Chem. Theor. Comput.* **2012**, *8*, 1212−1222. Siebert, M. R.; Zhang, J.; Addepalli, S. V.; Tantillo, D. J.; Hase, W. L. *J. Am. Chem. Soc.* **2011**, *133*, 8335−8343.

(32) (a) Mihailovic, M. M. Ph.D. Thesis Nr. 7535, ETH-Zurich, 1984. (b) Hanselmann, P., Ph.D. Thesis Nr. 8334, ETH-Zurich, 1987.